Magnetic Resonance Imaging

International Edition: DOI: 10.1002/anie.201507227
German Edition: DOI: 10.1002/ange.201507227

A Eu^{II}-Containing Cryptate as a Redox Sensor in Magnetic Resonance Imaging of Living Tissue

*Levi A. Ekanger, Lisa A. Polin, Yimin Shen, E. Mark Haacke, Philip D. Martin, and Matthew J. Allen**

Abstract: *The Eu^{II} ion rivals Gd^{III} in its ability to enhance contrast in magnetic resonance imaging. However, all reported Eu^{II}-based complexes have been studied in vitro largely because the tendency of Eu^{II} to oxidize to Eu^{III} has been viewed as a major obstacle to in vivo imaging. Herein, we present solid- and solution-phase characterization of a Eu^{II}-containing cryptate and the first in vivo use of Eu^{II} to provide contrast enhancement. The results indicate that between one and two water molecules are coordinated to the Eu^{II} core upon dissolution. We also demonstrate that Eu^{II}-based contrast enhancement can be observed for hours in a mouse.*

Magnetic resonance imaging (MRI) is a powerful diagnostic tool for imaging opaque tissues at relatively high spatial resolution and nearly unlimited depth penetration.[1] Paramagnetic complexes are routinely used as contrast agents in clinical MRI to provide contrast enhancement in areas of anatomical interest. For decades, Gd^{III} has been the paramagnetic metal ion of choice for contrast agents largely because it has seven unpaired electrons ($S = 7/2$) in an isotropic ground-state configuration ($^8S_{7/2}$). Eu^{II} is isoelectronic with Gd^{III}, and both ions enhance contrast in MRI.[2] Furthermore, the Eu^{II} center has a propensity to oxidize to Eu^{III}, resulting in a diamagnetic ground state ($^7F_0$) and a thermally accessible excited state ($^7F_1$) that do not noticeably enhance contrast in MRI.[3] Therefore, the oxidation of Eu^{II} offers the opportunity for metal-based redox-responsive contrast enhancement that is unachievable with Gd^{III}-based contrast agents. However, despite several groups exploring Eu^{II}-based complexes as contrast agents for MRI,[2–4] there has been no reported use of Eu^{II} in vivo. Herein, we report the first in vivo use of a Eu^{II}-containing cryptate. We also report characterization that reveals a discrepancy in the coordination environment of the complex between the solid and solution phases.

We chose to characterize and attempt in vivo imaging with Eu^{II}-222Fb (222Fb = 5,6-(4-fluorobenzo)-4,7,13,16,21,24-hexaoxa-1,10-diazabicyclo[8.8.8]hexacos-5-ene; Figure 1)

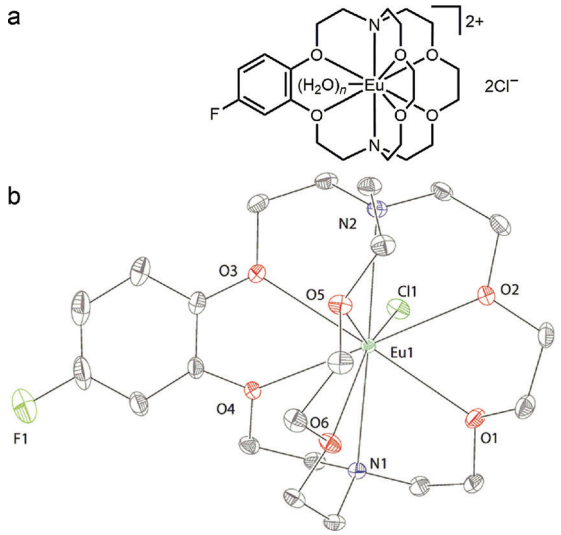

Figure 1. a) Proposed solution-phase structure of Eu^{II}-222Fb with non-coordinated chloride counterions and one or two coordinated water molecules ($n = 1$ or 2). b) X-ray crystal structure of Eu^{II}-222Fb with a coordinated chloride ion (hydrogen atoms and the outer-sphere chloride counterion are omitted for clarity).[15] *R* factor = 0.0248. Resolution = 0.59 Å. Thermal ellipsoids are set at 50% probability.

because it has a relatively positive oxidation peak potential (0.366 V versus the normal hydrogen electrode).[4f] More positive potentials favor the +2 oxidation state that is desirable for imaging. However, Eu^{II}-222Fb is prone to oxidation by molecular oxygen, and the Eu^{II} ion in this cryptate was expected to be oxidized to the Eu^{III} ion in tissues containing appreciable levels of molecular oxygen or other strong oxidants. In healthy tissue, intracellular environments tend to be reducing whereas extracellular environments tend to be oxidizing, but in necrotic tissue, dead cells leach components of the cytosol into the extracellular space to create a relatively reducing environment.[5] We hypothesized that the reducing environment of necrotic tissue would

[*] L. A. Ekanger, Prof. M. J. Allen
Department of Chemistry, Wayne State University
5101 Cass Avenue, Detroit, MI 48202 (USA)
E-mail: mallen@chem.wayne.edu
Homepage: http://chem.wayne.edu/allengroup
Prof. L. A. Polin
Department of Oncology, Wayne State University School of Medicine
110 East Warren Avenue, Detroit, MI 48201 (USA)
Dr. Y. Shen, Prof. E. M. Haacke
Department of Radiology, Wayne State University School of Medicine
3990 John R Street, Detroit, MI 48201 (USA)
Prof. L. A. Polin, Prof. E. M. Haacke, Prof. M. J. Allen
Barbara Ann Karmanos Cancer Institute
4100 John R Street, Detroit, MI 48201 (USA)
Dr. P. D. Martin
Lumigen Instrument Center
Chemistry Department, Wayne State University
5101 Cass Avenue, Detroit, MI 48202 (USA)

Supporting information for this article is available on the WWW under http://dx.doi.org/10.1002/anie.201507227.

prevent oxidation of Eu^{II}-222Fb and, consequently, contrast enhancement would be observed in necrotic tissue in the presence of Eu^{II}-222Fb. Before imaging in vivo, we characterized Eu^{II}-222Fb using solid- and solution-phase techniques.

The X-ray crystal structure of Eu^{II}-222Fb (Figure 1b) features a nine-coordinate metal center in an eclipsed hula-hoop-like geometry.[6] Eight coordination sites are occupied by six oxygen and two nitrogen atoms of 222Fb and the ninth site is occupied by a coordinated chloride counterion. Interestingly, this nine-coordinate geometry is different than the ten-coordinate geometry of a Sr^{II}-containing [2.2.2] cryptate (without the fluorobenzo group) that contains a coordinated water molecule and a coordinated trifluoromethanesulfonate anion.[4h] This difference is noteworthy because Sr^{II} and Eu^{II} have similar ionic radii, and Sr^{II} is often used as a diamagnetic analogue for Eu^{II}. As the coordination environment is a key parameter in the characterization of contrast agents for MRI, we investigated the coordination environment of Eu^{II}-222Fb in solution.

To test whether the chloride ion remained coordinated in solution, we measured the molar conductivity of Eu^{II}-222Fb in water. The molar conductivity was $211 \pm 1\ S\,cm^2\,mol^{-1}$, which is consistent with compounds exhibiting a 2:1 dissociation in water.[7] This observation indicates that, on average, no chlorides are coordinated to the Eu^{II} center in solution. However, because molar conductivity is a colligative property, it does not provide further information regarding the coordination environment of Eu^{II}-222Fb in solution.

To further characterize the coordination environment of Eu^{II}-222Fb in solution, we used variable-temperature ^{17}O NMR spectroscopy to investigate the coordination of water. Using 1% enriched $H_2{}^{17}O$ in phosphate-buffered saline, we were able to detect a paramagnetic broadening of the ^{17}O NMR signal upon addition of Eu^{II}-222Fb. The line broadening is consistent with the presence of inner-sphere water. This observation, coupled with a 2:1 dissociation, suggests that in solution Eu^{II}-222Fb is present either as a nine-coordinate species with chloride displaced by a water molecule or as a ten-coordinate species, based on the ability of Eu^{II} to adopt ten-coordinate geometries,[8] with two coordinated water molecules after chloride dissociation (Figure 2b). It is unlikely that more than two water molecules coordinate because 222Fb occupies eight coordination sites and to our knowledge, no eleven-coordinate molecular Eu^{II}-containing complexes have been reported. After studying the coordination environment of Eu^{II}-222Fb, we turned to in vitro MRI to characterize its ability to influence contrast.

To characterize the ability of Eu^{II}-222Fb to provide contrast enhancement, we measured the relaxivity of Eu^{II}-222Fb in phosphate-buffered saline using T_1-weighted MRI (T_1 = spin–lattice relaxation time). The relaxivity (24 °C, 7 T) of Eu^{II}-222Fb in phosphate-buffered saline was $6.5 \pm 0.3\ mM^{-1}\,s^{-1}$. Our measured relaxivity in phosphate-buffered saline is in agreement with other Eu^{II}-containing cryptates.[2b] Additionally, phosphate can bind lanthanide ions in a bidentate manner to displace two water molecules when the metal ion contains two adjacent coordinated water molecules.[9] Non-adjacent water would be consistent with water molecules replacing the two chloride ions (Figure 2b). The outer-sphere chloride is 5.383 Å from the Eu^{II} center (the coordinated chloride is 2.793 Å from Eu^{II}), and if both chloride ions are replaced by water molecules, a closer approach could be envisioned because of the smaller size of oxygen relative to chloride. Accordingly, our measured ^{17}O line broadening, crystal structure, and relaxivity suggest that if two water molecules are coordinated to Eu^{II}-222Fb in solution, that they are likely not adjacent to each other.

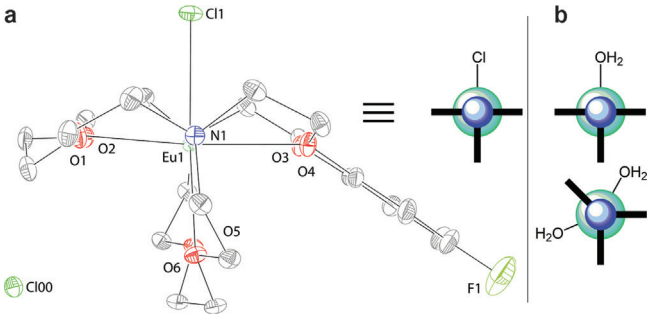

Figure 2. a) View of the X-ray crystal structure of Eu^{II}-222Fb[15] (along the N–Eu–N axis) of Eu^{II}-222Fb[15] (hydrogen atoms omitted for clarity) alongside a representation of the solid-phase geometry in the same orientation as the crystal structure. The outer-sphere chloride Cl00 related by symmetry is included in the image. b) Representation of the proposed solution-phase geometry of Eu^{II}-222Fb with one or two coordinated water molecules viewed along the N–Eu–N axis. The blue and green spheres in the models represent nitrogen and europium, respectively, and the bold lines represent the cryptands.

To test whether Eu^{II}-222Fb would enhance contrast in necrotic tissue, we performed T_1-weighted MRI before and after intratumoral injection of Eu^{II}-222Fb (50 μL, 19.4 mM) into a 4T1 mammary carcinoma. The 4T1 carcinoma model is an aggressive tumor that typically develops a necrotic core,[10] and imaging was performed when tumors reached approximately 700–1000 mg to maximize the probability of necrosis. Images were acquired before and at 3, 20, and 120 minutes after intratumoral injection (Figure 3a–d). Positive contrast enhancement was observed for the entirety of the 120 minute experiment, but the location of the positive contrast enhancement changed over time. Specifically, heterogeneous positive contrast enhancement was observed along nearly the entire length of the tumor immediately post injection, but was only observed in a localized core of the tumor after 120 minutes. These observations demonstrate that Eu^{II} persists within a tumor for at least 120 minutes. We detected this duration of positive contrast enhancement in all seven of our imaging experiments with independently injected tumors. The presence of contrast enhancement is consistent with the persistence of the +2 oxidation state of europium in the core of the tumor, and the reduced oxidation state is suggestive of a lack of oxygen.

To verify the presence of necrotic tissue in the tumor, we sacrificed the mouse directly after the 120 minute post-injection image and performed histological staining. The tumor was removed in whole, fixed in formalin, mounted in paraffin, and cut to a thickness of 5 μm before being stained with hematoxylin and eosin (Figure 3f). Hematoxylin is a dye that stains nuclei, and eosin stains elements of the cytoplasm

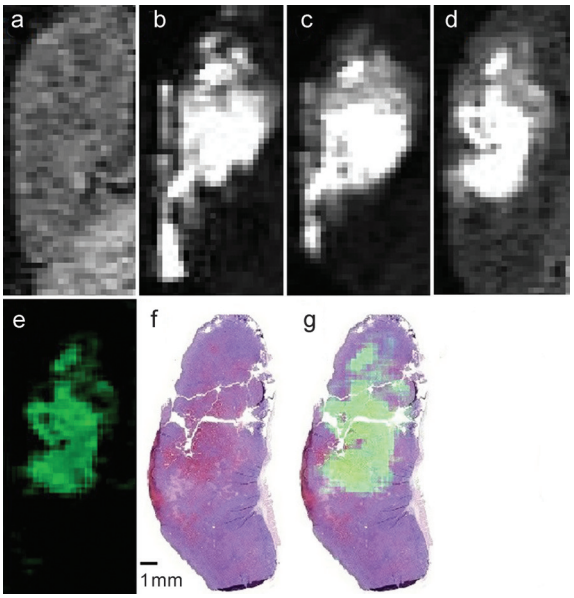

Figure 3. T_1-weighted in vivo sagittal plane images of a 4T1 tumor injected with Eu^{II}-222Fb. Images are recorded a) pre-injection and b) 3 min, c) 20 min, and d) 120 min post-intratumoral injection. e) The difference between the 120 min and pre-injection images (image (d) minus image (a)) colored using the ImageJ green lookup table. f) Hematoxylin- and eosin-stained slice of the tumor imaged in (a–e) and g) the sum of images (e) and (f). All images are on the same scale. Selected imaging parameters: echo time = 1.5 ms, repetition time = 11 ms, flip angle = 40°, field of view = 30 mm × 90 mm, in-plane resolution = 0.352 mm × 0.352 mm.

as a counterstain to differentiate areas that are nuclei-abundant (blue) from those that are nuclei-deficient (pink).[11] Areas associated with necrosis are expected to stain pink to a greater extent than non-necrotic areas because of the lack of cells and their corresponding nuclei in necrotic regions. The stained slice revealed nuclei-deficient regions consistent with necrosis that were particularly pronounced in the mid-to-upper half of the tumor. The leftmost region of the slice stained pink from the presence of tumor ulceration through the mouse epidermis. Consistent with staining, the majority of positive contrast enhancement observed 120 minute post-injection was in the mid-to-upper half of the tumor, suggesting that Eu^{II}-222Fb provided positive contrast enhancement in the necrotic core of the tumor (Figure 3g). No contrast enhancement was observed in the leftmost region of the tumor likely because of direct contact between tumor ulceration and oxygen in the air. It is worth reiterating that we used an intratumoral injection, which may have placed a bolus in the tumor core and the lack of oxygen allowed Eu^{II} to persist.

To better understand the potential mechanism of differentiation, we performed an intratumoral injection of Eu^{II}-222Fb (50 μL, 6.9 mM) and monitored contrast enhancement over the course of 3 h before sacrificing the mouse and removing the injected tumor for analysis of Eu content by inductively coupled plasma mass spectrometry. At 3 h post injection, we detected a decrease in positive contrast enhancement (circa 85 %) in the tumor relative to the initial image and a decrease in the Eu content (circa 80 %) in the tumor relative to the injected dose. These close values suggest clearance of Eu^{II}-222Fb played a major role in the loss of positive contrast enhancement. Clearance was not directly observed in T_1-weighted MRI because Eu^{II}-222Fb likely oxidized in tissues or fluids of relatively higher oxygen content, and the product of oxidation, Eu^{III}, does not produce positive contrast enhancement. Furthermore, when Gd^{III}-1,4,7,10-tetraazacyclododecane-1,4,7,10-tetraacetate (50 μL, 20.5 mM) was injected into a tumor in a separate experiment, the bladder of the mouse was bright with contrast within minutes of the injection. We observed this phenomenon in two independently injected tumors. This non-redox-active control indicates that the concentration of the Eu^{II} complex injected should be enough to visualize in the bladder if clearance occurred without oxidation. The evidence of clearance based on Eu content and the lack of contrast enhancement observed outside of the tumor demonstrates the lack of background enhancement possible with Eu^{II}-based imaging agents in redox-active environments. Although the connection between positive contrast enhancement and necrotic tissue is intriguing, more detailed experiments are required to evaluate the nature of Eu^{II}-222Fb clearance over time. Regardless of the mechanism of differentiation, our in vivo imaging data demonstrate the first reported use of Eu^{II}-based compounds for in vivo contrast-enhanced MRI.

To investigate the in vitro stability of Eu^{II}-222Fb with respect to oxygen exposure, we measured the T_1 value (37 °C, 1.4 T) of Eu^{II}-222Fb in phosphate-buffered saline to monitor the oxidation of Eu^{II} as a function of air exposure while stirring. Under an atmosphere of N_2 ($p(O_2) \approx 0$ mmHg; p = partial pressure), Eu^{II}-222Fb remained in the +2 oxidation state for at least 118 days. However, upon stirring in open air ($p(O_2) \approx 160$ mmHg), the observed T_1 enhancement was completely lost within 5 minutes. This rapid oxidation with elevated oxygen exposure suggests that Eu^{II}-222Fb is oxidized upon clearance from the oxygen-deficient 4T1 necrotic core ($p(O_2) \leq 10$ mmHg)[12,13] into relatively oxygenated vasculature ($p(O_2) \approx 40$–100 mmHg).[14] Collectively, the persistence of the +2 oxidation state over a 120 minute period, the correlation between necrotic tissue and contrast enhancement, the lack of positive contrast enhancement in organs associated with clearance (bladder, liver, or kidneys), and the rapid oxidation observed with elevated air exposure suggest that Eu^{II}-222Fb persists in the poorly oxygenated necrotic core of the tumors and oxidizes elsewhere.

In conclusion, we report solid- and solution-phase characterization of the complex Eu^{II}-222Fb that is nine-coordinate in the solid state and nine- or ten-coordinate in solution. Additionally, we report the first in vivo contrast-enhanced MRI with a Eu^{II}-based contrast agent, and efforts are underway in our laboratory to understand the behavior of Eu^{II}-222Fb in vivo. We expect that the ability to differentiate necrotic from non-necrotic tissue in vivo coupled with the tunable oxidation potential of the Eu^{II} core will enable bracketing of tissue redox environments associated with both hypoxic and hyperoxic tissues relevant to the study of many diseases.

Acknowledgements

The authors acknowledge the National Institutes of Health (NIH) for support (R01EB013663). The Biobanking and Correlative Sciences Core and the Animal Model and Therapeutics Evaluation Core are supported, in part, by an NIH Center grant (P30CA022453) to the Barbara Ann Karmanos Cancer Institute at Wayne State University (WSU). The authors are grateful to WSU for a Thomas C. Rumble Graduate Research Fellowship (L.A.E.) and a Schaap Faculty Scholar Award (M.J.A.).

Keywords: cryptands · europium · imaging agents · magnetic resonance imaging · structure elucidation

How to cite: *Angew. Chem. Int. Ed.* **2015**, *54*, 14398–14401
Angew. Chem. **2015**, *127*, 14606–14609

[1] a) G. Radecki, R. Nargeot, I. O. Jelescu, D. Le Bihan, L. Ciobanu, *Proc. Natl. Acad. Sci. USA* **2014**, *111*, 8667–8672; b) S. J. van Veluw, J. J. M. Zwanenburg, J. Engelen-Lee, W. G. M. Spliet, J. Hendrikse, P. R. Luijten, G. J. Biessels, *J. Cereb. Blood Flow Metab.* **2013**, *33*, 322–329.

[2] a) L. A. Ekanger, M. J. Allen, *Metallomics* **2015**, *7*, 405–421; b) J. Garcia, J. Neelavalli, E. M. Haacke, M. J. Allen, *Chem. Commun.* **2011**, *47*, 12858–12860.

[3] L. A. Ekanger, M. M. Ali, M. J. Allen, *Chem. Commun.* **2014**, *50*, 14835–14838.

[4] a) M. Regueiro-Figueroa, J. L. Barriada, A. Pallier, D. Esteban-Gómez, A. de Blas, T. Rodríguez-Blas, É. Tóth, C. Platas-Iglesias, *Inorg. Chem.* **2015**, *54*, 4940–4952; b) A. N. W. Kuda-Wedagedara, C. Wang, P. D. Martin, M. J. Allen, *J. Am. Chem. Soc.* **2015**, *137*, 4960–4963; c) M. Gál, F. Kielar, R. Sokolová, Š. Ramešová, V. Kolivoška, *Eur. J. Inorg. Chem.* **2013**, *2013*, 3217–3223; d) J. Garcia, M. J. Allen, *Inorg. Chim. Acta* **2012**, *393*, 324–327; e) J. Garcia, A. N. W. Kuda-Wedagedara, M. J. Allen, *Eur. J. Inorg. Chem.* **2012**, *2012*, 2135–2140; f) N.-D. H. Gamage, Y. Mei, J. Garcia, M. J. Allen, *Angew. Chem. Int. Ed.* **2010**, *49*, 8923–8925; *Angew. Chem.* **2010**, *122*, 9107–9109; g) L. Burai, É. Tóth, G. Moreau, A. Sour, R. Scopelliti, A. E. Merbach, *Chem. Eur. J.* **2003**, *9*, 1394–1404; h) L. Burai, R. Scopelliti, É. Tóth, *Chem. Commun.* **2002**, 2366–2367; i) P. Caravan, É. Tóth, A. Rockenbauer, A. E. Merbach, *J. Am. Chem. Soc.* **1999**, *121*, 10403–10409.

[5] a) M. T. Lotze, H. J. Zeh, A. Rubartelli, L. J. Sparvero, A. A. Amoscato, N. R. Washburn, M. E. DeVera, X. Liang, M. Tör, T. Billiar, *Immunol. Rev.* **2007**, *220*, 60–81; b) A. Rubartelli, M. T. Lotze, *Trends Immunol.* **2007**, *28*, 429–436.

[6] A. Ruiz-Martínez, D. Casanova, S. Alvarez, *Chem. Eur. J.* **2008**, *14*, 1291–1303.

[7] A. Apelblat, M. A. Esteso, M. Bešter-Rogač, *J. Phys. Chem. B* **2013**, *117*, 5241–5248.

[8] J. Christoffers, P. Starynowicz, *Polyhedron* **2008**, *27*, 2688–2692.

[9] R. M. Supkowski, W. D. Horrocks, *Inorg. Chem.* **1999**, *38*, 5616–5619.

[10] K. Tao, M. Fang, J. Alroy, G. G. Sahagian, *BMC Cancer* **2008**, *8*, 228.

[11] K. Degenhardt, R. Mathew, B. Beaudoin, K. Bray, D. Anderson, G. Chen, C. Mukherjee, Y. Shi, C. Gélinas, Y. Fan, D. A. Nelson, S. Jin, E. White, *Cancer Cell* **2006**, *10*, 51–64.

[12] M. E. Hardee, M. W. Dewhirst, N. Agarwal, B. S. Sorg, *Curr. Mol. Med.* **2009**, *9*, 435–441.

[13] M. K.-S. Leow, *Adv. Physiol. Educ.* **2007**, *31*, 198–201.

[14] A. Carreau, B. E. Hafny-Rahbi, A. Matejuk, C. Grillon, C. Kieda, *J. Cell. Mol. Med.* **2011**, *15*, 1239–1253.

[15] CCDC 1415606 ([Eu^{II}-222FbCl]Cl) contains the supplementary crystallographic data for this paper. These data are provided free of charge by The Cambridge Crystallographic Data Centre.

Received: August 3, 2015
Revised: August 25, 2015
Published online: October 2, 2015

